Mechanism of thioamide drug action against tuberculosis and leprosy

Feng Wang,[1] Robert Langley,[1] Gulcin Gulten,[1] Lynn G. Dover,[3] Gurdyal S. Besra,[3] William R. Jacobs Jr.,[2] and James C. Sacchettini[1]

[1]Department of Biochemistry and Biophysics, Texas A&M University, College Station, TX 77843
[2]Howard Hughes Medical Institute, Department of Microbiology and Immunology, Albert Einstein College of Medicine of Yeshiva University, Bronx, NY 10461
[3]School of Biosciences, University of Birmingham, Birmingham B15 2TT, England, UK

Thioamide drugs, ethionamide (ETH) and prothionamide (PTH), are clinically effective in the treatment of *Mycobacterium tuberculosis*, *M. leprae*, and *M. avium* complex infections. Although generally considered second-line drugs for tuberculosis, their use has increased considerably as the number of multidrug resistant and extensively drug resistant tuberculosis cases continues to rise. Despite the widespread use of thioamide drugs to treat tuberculosis and leprosy, their precise mechanisms of action remain unknown. Using a cell-based activation method, we now have definitive evidence that both thioamides form covalent adducts with nicotinamide adenine dinucleotide (NAD) and that these adducts are tight-binding inhibitors of *M. tuberculosis* and *M. leprae* InhA. The crystal structures of the inhibited *M. leprae* and *M. tuberculosis* InhA complexes provide the molecular details of target–drug interactions. The purified ETH-NAD and PTH-NAD adducts both showed nanomolar K_is against *M. tuberculosis* and *M. leprae* InhA. Knowledge of the precise structures and mechanisms of action of these drugs provides insights into designing new drugs that can overcome drug resistance.

CORRESPONDENCE
James C. Sacchettini:
sacchett@tamu.edu

Thioamide drugs, ethionamide (ETH) and prothionamide (PTH), have been widely used for many years in the treatment of mycobacterial infections caused by *Mycobacterium tuberculosis*, *M. leprae*, and *M. avium* complex infections (1, 2). ETH and PTH are both bacteriocidal and are essentially interchangeable in a chemotherapy regimen. They are the most frequently used drugs for the treatment of drug-resistant tuberculosis and, therefore, are becoming increasingly relevant as the number of multidrug-resistant and extensively drug-resistant cases is increasing worldwide (3, 4). Moreover, ETH and PTH are also used in a combined chemotherapy regimen with either dapsone or rifampin to treat leprosy (5). Although we have previously speculated about the mechanism of action of ETH in *M. tuberculosis* based on an analogy to isoniazid's (INH's) mode of action (6–8), definitive biochemical evidence that ETH targets InhA has not been forthcoming.

ETH and PTH are structurally similar to INH (Fig. 1), and it is clear that all of these drugs inhibit mycolic acid biosynthesis (9, 10). It was demonstrated that a single amino acid mutation of *inhA*, S94A, was sufficient to confer resistance to both ETH and INH in *M. smegmatis*, *M. bovis* (6, 11), and *M. tuberculosis* (8). Moreover, overexpression of *inhA* conferred resistance to both INH and ETH in *M. tuberculosis*, *M. bovis*, and *M. smegmatis* (12). Indeed, several *M. tuberculosis* clinical isolates resistant to INH contain mutations in the *inhA* gene, and all have been found to be cross-resistant to ETH (13). These observations genetically demonstrated that the primary target of both INH and ETH was InhA, the enoyl-acyl ACP reductase involved in mycolic acid biosynthesis. In addition, subsequent biochemical analysis has clearly shown that the primary molecular target of INH is InhA (7, 8, 14–16).

INH is a prodrug that requires activation by KatG, a catalase-peroxidase (17, 18), to form an adduct with nicotinamide adenine dinucleotide (NAD^+). It is the isonicotinic-acyl-NAD adduct that inhibits InhA (7, 8, 16). Although ETH is also a prodrug that requires activation to exert antitubercular activity, KatG mutant strains resistant to INH are sensitive to ETH, indicating that ETH has a different activator

The online version of this article contains supplemental material.

(13, 19). Mutations of a gene designated *ethA* were repeatedly found in the clinical isolates resistant to ETH (13, 20). Like KatG, the overexpression of *ethA* in *M. smegmatis* resulted in substantially increased ETH sensitivity (21). This evidence suggested that *ethA* is critical for the activation of ETH.

ethA encodes a flavin monooxygenase found to catalyze the Baeyer-Villiger reaction to detoxify aromatic and long-chain ketones (22). The enzyme is membrane associated and has a tendency to form large oligomers after purification (22, 23). The monooxygenase activity of the purified EthA is very low (k_{cat} = 0.00045 s^{-1}), suggesting that the enzyme may require other proteins or cellular components to be completely functional (22). The active form of ETH has never been detected or isolated in vitro, although some inactive metabolites produced by the catalytic oxidation of ETH by EthA have been studied by TLC and HPLC (20).

RESULTS AND DISCUSSION

To identify the active form of ETH, we and others have attempted to use purified EthA to activate ETH and inhibit InhA in vitro but have never been able to observe any InhA inhibition (unpublished data). Because in vitro activation of the drugs ETH and PTH has not been possible by either chemical or enzymatic approaches, we developed a cell-based activation method. In this system, recombinant *M. tuberculosis* EthA and InhA were co-overexpressed in the same *Escherichia coli* cell, and ETH or PTH was added to the culture to test whether the drugs would inhibit InhA upon activation. Although ETH and PTH are both potent drugs against *M. tuberculosis* (MIC = ~0.5 μg/ml) (24), they do not affect *E. coli* growth, even at very high concentrations (100 μg/ml), which is primarily caused by the absence of an EthA homologue in *E. coli*.

InhA and EthA from *M. tuberculosis* were coexpressed in *E. coli* BL21 (DE3) in the presence of 100 μg/ml ETH. InhA was rapidly purified, and an in vitro enzyme assay was performed. InhA isolated from the experimental sample had <1% of the specific activity of InhA purified without the addition of ETH under the same assay condition. Mass analysis of denatured InhA from the experimental sample indicated the presence of a small molecule with a molecular weight of 798.2 (Fig. S1, A and B, available at http://www.jem.org/cgi/content/full/jem.20062100/DC1). This corresponds to the exact molecular weight of an ethyl- isonicotinic-acyl-NAD covalent adduct. Moreover, pure fractions of this small

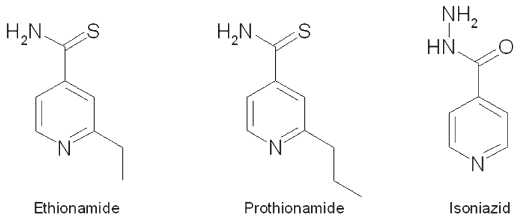

Figure 1. Chemical structure of ETH, PTH, and INH. Although these prodrugs have similar structures, INH is activated by a catalase-peroxidase, whereas ETH and PTH are activated by a flavin-dependent monooxygenase.

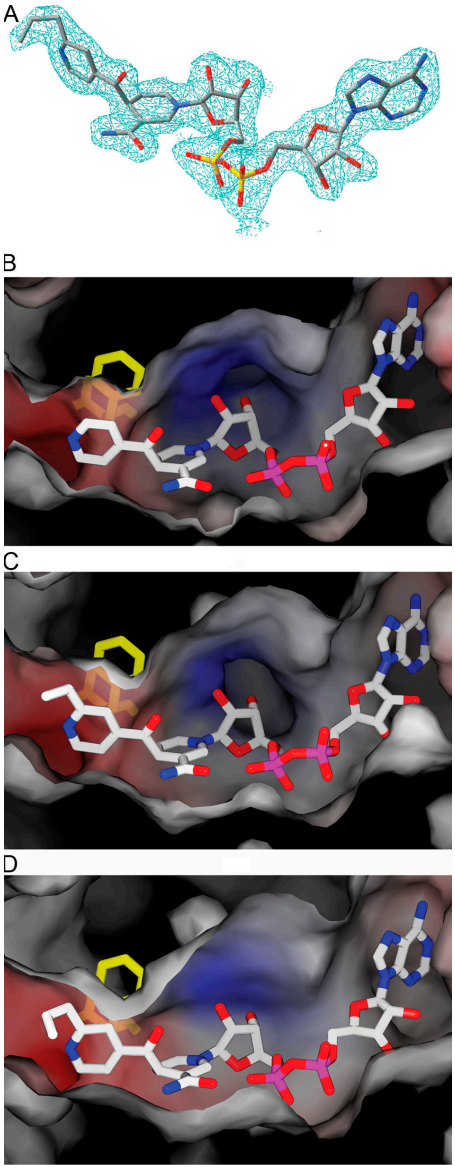

Figure 2. Active sites of the *M. tuberculosis* enoyl–acyl ACP reductases bound to inhibitors and the bound inhibitor. (A) The crystal structure of PTH-NAD superimposed onto the simulated annealing omit electron density map contoured at 1 σ. Carbon atoms are gray, oxygen atoms are red, nitrogen atoms are blue, and phosphor atoms are orange. The 2-propyl-isonicotinic acyl group is covalently attached to the 4 position of the nicotinamide ring of NADH in a 4S configuration. (B) Cross section through the surface of the InhA active site with bound INH-NAD. (C) Cross section through the surface of the InhA active site with bound ETH-NAD showing that the 2-ethyl-isonicotinic acyl moiety protrudes into a hydrophobic binding pocket created by the rearrangement of the side chain of Phe^{149} (shown behind the transparent surface), which is similar to INH-NAD. (D) Cross section through the surface of the InhA active site with bound PTH-NAD, which has a similar binding mode to INH-NAD and ETH-NAD. The carbon atoms of the adduct inhibitors and Phe^{149} are white and yellow, respectively.

molecule showed strong inhibition to native InhA in vitro (Ki = 7 ± 5 nM), which is as potent as the INH-NAD adduct, the active form of INH (Ki = 5 nM) (8). When PTH was used in the same coexpression experiment, a compound with a molecular weight of 812.2 was identified that corresponds to the exact weight of a propyl-isonicotinic-acyl-NAD adduct (Fig. S1 C). This compound is also extremely potent against InhA in vitro (Ki = 2 ± 0.8 nM).

M. tuberculosis InhA in complex with the adducts was crystallized. X-ray diffraction data to 2.2 and 2.5 Å resolution were collected from single crystals of ETH and PTH complexes, respectively (Table S1, available at http://www.jem.org/cgi/content/full/jem.20062100/DC1). Unbiased electron density maps of each complex clearly indicated the presence of a modified NAD with an ethyl-isonicotinic-acyl or propyl-isonicotinic-acyl group covalently attached to the 4 position of the nicotinamide ring in a 4S configuration (Fig. 2 A). The chemical structures of both inhibitors are consistent with the molecular weights obtained by the mass analysis. Similar to the structure of InhA bound with the adduct INH-NAD (7), the ethyl-isonicotinic-acyl, or the propyl-isonicotinic-acyl, moiety is found in a hydrophobic pocket that was formed by the rearrangement of the side chain of Phe^{149} (Fig. 2, B–D). The ethyl-isonicotinic acyl or the propyl-isonicotinic-acyl group also forces the side chain of Phe^{149} to rotate ~90°, forming an aromatic ring-stacking interaction with the pyridine ring (Fig. 3 A). The pocket is predominantly lined by hydrophobic groups from the side chains of Tyr^{158}, Phe^{149}, Met^{199}, Trp^{222}, Leu^{218}, Met^{155}, Met^{161}, and Pro^{193}, and is adjacent and partly overlapped with the fatty acyl substrate-binding site. Indeed, the atoms common to ETH-NAD, PTH-NAD, and INH-NAD are in nearly identical positions. The only difference is the extra ethyl or propyl group at the 2 position of the pyridine ring of ETH or PTH. The ethyl group contributes to the binding of ETH-NAD adduct by forming π-stacking interactions with the aromatic side chain of Tyr^{158} at a distance of ~3.3 Å. It is also within van der Waal interaction distances with side chains of Leu^{218} (3.3 Å) and Met^{155} (3.2 Å). The hydrogen-bonding interactions between the phosphate group of the adduct and residues of the nucleotide-binding site are well conserved. Therefore, it is very likely that mutations, such as S94A, that decrease the binding of NAD(H) and the INH-NAD adduct would also weaken the binding of ETH-NAD and PTH-NAD (Fig. 4). This explains why the S94A mutant strain of *M. tuberculosis* is coresistant to both INH and ETH.

Other than ETH and PTH, thioamide drugs such as thiacetazone and isoxl have been shown to be activated by EthA (20). The same cell-based method was applied to test thiacetazone. The isolated InhA was not inhibited under the same assay condition. As expected, mass analysis did not show the existence of any tightly bound inhibitor. These results indicate that, unlike ETH or PTH, thiacetazone does not target InhA, even though all of these thioamides are activated by EthA in *M. tuberculosis*.

Unlike INH, which is not effective against *M. leprae*, most likely because of the dysfunction of *M. leprae katG*, ETH and PTH are used in the treatment of leprosy. Genome

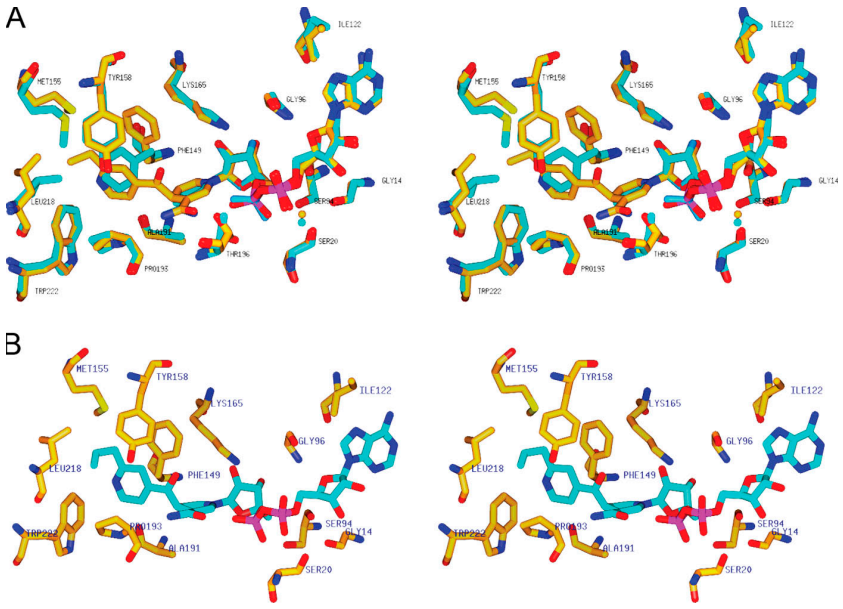

Figure 3. *M. tuberculosis* InhA with bound inhibitors. (A) Stereo view of the superposition of active sites of the *M. tuberculosis* InhA:NADH structure and the InhA:ETH-NAD structure, showing the side chain of Phe^{149} rotated ~90° once the ETH-NAD adduct binds to the enzyme. The carbon atoms of residues and NADH in the InhA:NADH structure are cyan. The carbon atoms of residues and ETH-NAD in the InhA:ETH-NAD structure are gold. (B) The stereo view of the active sites of the *M. leprae* InhA:PTH-NAD structure. The carbon atoms of residues and PTH-NAD adduct are gold and cyan, respectively. Other atoms are colored according to the atom type (red, oxygen atoms; blue, nitrogen atoms; yellow, sulfur atoms; and orange, phosphor atoms).

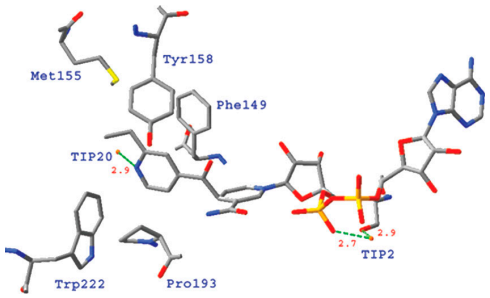

Figure 4. Selected interactions between ETH-NAD and the active site of InhA. A conserved water molecule, TIP20, forms a hydrogen bond interaction with the nitrogen atom of the 2-ethyl-isonicotinic acyl moiety of the inhibitor at a distance of 2.9 Å. The other water molecule, TIP2, is in the center of a hydrogen bonding network, which interacts with the oxygen atom of the phosphate group of the adduct and the hydroxyl group of Ser^{94} at distances of 2.7 and 2.9 Å, respectively.

analysis indicated that both *M. leprae* and *M. avium* have *ethA* and *inhA* homologues with high sequence similarities to their *M. tuberculosis* counterparts. Therefore, the *M. leprae ethA* and *inhA* were coexpressed, in the presence of PTH using a cell-based activation method similar to *M. tuberculosis*, as described in the second paragraph in Results and discussion. A compound with the same molecular weight as PTH-NAD adduct was identified, which also showed strong inhibition to *M. leprae* InhA (Ki = 11 ± 6 nM) in vitro.

The crystal structure of *M. leprae* InhA in complex with PTH-NAD was solved to 2.1 Å resolution to compare the binding mode of the inhibitor with the enzyme with *M. tuberculosis* InhA. The overall structure of *M. leprae* InhA is similar to *M. tuberculosis* InhA (RMSD = 1.3 Å for C_αs), and the active site residues are conserved. The propyl-isonicotinic-acyl moiety of the adduct is observed inside a hydrophobic pocket. The pyridyl ring forms a π-stacking interaction with the aromatic side chain of Phe^{149}, and the propyl group is π stacking with the aromatic side chain of Tyr^{158}. Residues, including Ser^{94} in the nucleotide-binding site, form hydrogen-bonding interactions with the phosphate group of the adduct in a similar manner as *M. tuberculosis* InhA (Fig. 3 B). These results supported our hypothesis that the active form of PTH inhibits *M. leprae* InhA in a similar way to *M. tuberculosis* InhA. Although no clinical or experimental mutant of *M. leprae* InhA has been reported thus far, based on the binding mode of the PTH-NAD adduct, it is very likely that the mutations of InhA found in ETH-resistant *M. tuberculosis* mutant strains, such as S94A, would also confer resistance of *M. leprae* to ETH and PTH.

Although ETH and INH NAD adducts are similar, their activation mechanisms are very different. INH, a hydrazid, is activated by the heme-using catalase-peroxidase KatG (16, 18). We proposed that INH was oxidized to generate an isonicotinic-acyl free radical, which subsequently attacked the NAD^+ to form INH-NAD (7). ETH, a thioamide, has been shown to be metabolized by EthA, a FAD enzyme found in *M. tuberculosis*. It has been proposed that a free radical metabolite

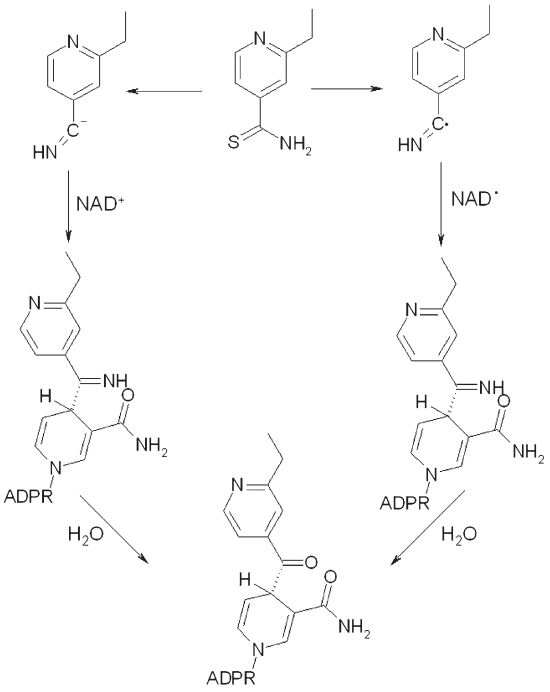

Figure 5. Possible reaction mechanisms for the activation of ETH and the formation of ETH-NAD. Two plausible mechanisms for the activation of ETH are shown. Either route will lead to the observed ETH-NAD adduct, retaining a tetrahedral carbon at position 4 of the nicotinamide ring.

intermediate could be generated through EthA oxidation of ETH, similar to the activation of INH. However, no active species that inhibit InhA were isolated in vitro (20), which suggests that an unknown cell component, either a protein or cell membrane, is required for the formation of the adduct by the free radical intermediate. We believe that the inactive metabolites isolated in previous attempts could result from side reactions and quenching of the free radical intermediate in solution. It is still not clear how the thioamide is oxidized by EthA. Tokuyama et al. demonstrated that a thioamide could be used as a precursor of a synthon equivalent to an imidoyl radical in converting thioamides to corresponding indole derivatives. Bu_3SnH/Et_3B has been used as a free radical initiator in pure organic solvent (25). Similarly, we postulate that ETH is converted to an imidoyl radical, and this imidoyl radical subsequently attacks NAD^+ to form an adduct, which is then converted to ethyl-isonicotinic-acyl-NAD adduct after hydrolysis to release the amine group. It is also possible that the imidoyl anion is the intermediate before forming the adduct with NAD (Fig. 5). However, based on the current evidence, we are not certain if this reaction is catalyzed by EthA alone or requires the involvement of additional enzymes.

The experiments presented in this paper describe the molecular mechanism of the drug action of ETH and PTH against *M. tuberculosis* and *M. leprae*. The identification of the

ETH-NAD and PTH-NAD adducts, like the INH-NAD, represent a novel paradigm in the history of drug action. Efforts to detect the INH-NAD and ETH-NAD adduct in *M. tuberculosis* or other mycobacteria have been unsuccessful. However, four different mechanisms of coresistance to INH and ETH have been discovered: (a) overexpression of the InhA target (6, 12); (b) target modification to prevent adduct binding (8); (c) activator modification to prevent prodrug activation and adduct formation (20); and (d) mutations in *ndh*, the gene encoding the essential NADH dehydrogenase II that regulates intracellular NADH/NAD ratios (26). All of these observations are consistent with our working model that INH, ETH, and PTH are all prodrugs that form NAD adducts to inhibit InhA. The discovery of ETH-NAD and PTH-NAD adducts, which are generated through completely different routes from INH-NAD, further validates this model. This information is important for the optimization of drug activity and the understanding of drug resistance. Because the molecular target of ETH, PTH, and INH is the same, it validates InhA as an outstanding antituberculosis and antileprosy drug target. However, because most of the clinical strains resistant to ETH and PTH contain mutations in the *ethA* gene, it is advantageous to find agents that inhibit InhA, without the need for EthA activation, as effective chemotherapy against resistant bacteria.

MATERIALS AND METHODS

Cloning, expression, and purification. The *M. tuberculosis inhA* has been previously cloned (14). *M. tuberculosis ethA* was cloned from genomic DNA (National Institutes of Health contract N01-AI-75320; Colorado State University). The amplified product was inserted into pET28b using the NdeI and NotI restriction sites. *M. leprae ethA* and *inhA* were cloned from genomic DNA. The amplified product of *M. leprae ethA* was inserted into pET15b using the NdeI and BamHI restriction sites. *M. leprae inhA* was inserted into pET30b using the NdeI and HindIII restriction sites.

The plasmids of *M. tuberculosis inhA* and *ethA* were singly and doubly transformed into *E. coli* BL21 (DE3; EMD Biosciences, Inc.). The strain containing plasmids of *inhA* and *ethA* was cultured in LB-Miller media containing 50 μg/ml kanamycin and 50 μg/ml carbanicillin at 37°C until OD_{600} reached 0.8. Expression of both genes was induced for 20 h at 16°C by addition of 1 mM isopropyl β-D-thiogalactopyranoside. At the same time as induction, 100 μg/ml ETH or PTH was also added to the culture. The same protocol was used for the strain containing only the *inhA* plasmid.

Recombinant InhA was purified according to the previous method (14).

The coexpression and purification of *M. leprae ethA* and *inhA* were conducted using protocols similar to those used for the *M. tuberculosis* enzymes.

Isolation and characterization of ETH-NAD and PTH-NAD. InhA purified from the experimental strain containing both *inhA* and *ethA* genes was concentrated and heated for 40 s at 100°C. After the heat treatment, ETH-NAD or PTH-NAD was separated from denatured enzymes by filtration, using a centricon device (cutoff size = 30 kD). The concentration of ETH-NAD and PTH-NAD was determined by its absorbance at 260 and 326 nM (16). The molecular weight of both adducts was determined by matrix-assisted laser desorption/ionization (MALDI) performed on an ABI Voyager-DE STR (AME Bioscience): ETH-NAD, calculated weight = 797.2 and found weight = 797.3 (negative mode), and calculated weight = 799.2 and found weight = 799.2 (positive mode); PTH-NAD, calculated weight = 811.2 and found weight = 811.3 (negative mode).

InhA enzymatic activity assay. All assays were performed on a spectrophotometer (Cary 100 Bio Spectrophotometer; Varian, Inc.) at 25°C by monitoring oxidation of NADH at 340 nm. Reactions were initiated by adding 50 μM of substrate dodecenoyl-CoA to assay mixtures containing 1 nM InhA, 100 μM NADH, and 3–2,000 nM of adduct inhibitors.

The IC_{50} was determined from the dose-response plot of enzyme fractional activity as a function of inhibitor concentration. K_i was obtained by dividing the IC_{50} value by $1 + [S_1]/K_{m1} + [S_2]/K_{m2}$, where $[S_1]$ and $[S_2]$ are the concentrations of dodecenoyl-CoA and NADH, and K_{m1} and K_{m2} are their Michaelis constants.

Crystallization of InhA in complex with ETH-NAD adduct. Crystallization was accomplished by the hanging drop vapor diffusion method (27). *M. tuberculosis* InhA in complex with inhibitors was cocrystallized in hanging droplets containing 2 μl of protein solution at 10 mg/ml and 2 μl of buffer (12% MPD, 4% DMSO, 0.1 M Hepes, 0.025 M sodium citrate) at 16°C in Linbro plates against 1 ml of the same buffer. Diamond-shaped protein crystals formed ~4 d later.

M. leprae InhA in complex with inhibitor was cocrystallized in a similar manner, and the crystal had a cubic shape.

Data collection and processing. Data were collected at 121 K using cryoprotection solution containing reservoir solution with an additional 30% MPD. Crystals of *M. tuberculosis* InhA:ETH-NAD and *M. leprae* InhA:PTH-NAD diffracted x rays to 2.2 and 1.8 Å using the beamline 23-ID at the Advanced Photon Source (Argonne National Laboratory, Argonne, IL). Diffraction data were collected from a single crystal with 1° oscillation widths for a range of 120°. Crystals of *M. tuberculosis* InhA:PTH-NAD were diffracted to 2.5 Å using a Raxis image plate detector coupled to a Rigaku x-ray generator using a copper rotating anode (CuK_α, $\lambda = 1.54$ Å). The data were integrated and reduced using HKL-2000 (HKL Research, Inc.; Table S1) (28).

Structure determination and model refinement. Crystals produced from InhA in complex with ETH-NAD were isomorphous to those of the native enzyme. Initial phases were obtained by molecular replacement using the apo-InhA structure (1ENY) and refined with CNS software (Table S1) (29). $F_o - F_c$ and $2F_o - F_c$ electron density maps were calculated, and an additional density resembling the inhibitor was found. The ligand was fit into the additional density, and the whole model was rebuilt using XtalView (30). During the final cycles of the refinement, water molecules were added into peaks above 3 σ of the $F_o - F_c$ electron density maps that were within hydrogen-bonding distances from the appropriate protein atoms. The final refinement statistics are listed in Table S1.

Online supplemental material. Table S1 provides data collection, processing, and refinement statistics. Fig. S1 depicts MALDI mass spectra showing that two inhibitors bound to InhA are compounds with the apparent weights of 798 and 812, respectively. Fig. S2 shows the crystal structure of the adducts superimposed onto the simulated annealing omit electron density maps contoured at 1 and 1.5 σ. Online supplemental material is available at http://www.jem.org/cgi/content/full/jem.20062100/DC1.

We thank Shane Tichy for his excellent technical assistance in mass spectrometry.

This work was supported by National Institutes of Health grant PO1AI068135, Einstein/MMC Center for AIDS Research grants AI51519 and AI43268, and by the Robert A. Welch Foundation. G.S. Besra acknowledges support from Mr. James Bardrick in the form of a Personal Research Chair and from the Medical Research Council.

The authors have no conflicting financial interests.

Submitted: 2 October 2006
Accepted: 19 December 2006

REFERENCES

1. Fajardo, T.T., R.S. Guinto, R.V. Cellona, R.M. Abalos, E.C. Dela Cruz, and R.H. Gelber. 2006. A clinical trial of ethionamide and

prothionamide for treatment of lepromatous leprosy. *Am. J. Trop. Med. Hyg.* 74:457–461.
2. Yajko, D.M., P.S. Nassos, and W.K. Hadley. 1987. Therapeutic implications of inhibition versus killing of *Mycobacterium avium* complex by antimicrobial agents. *Antimicrob. Agents Chemother.* 31:117–120.
3. Centers for Disease Control and Prevention. 2006. Emergence of *Mycobacterium tuberculosis* with extensive resistance to second-line drugs–worldwide, 2000-2004. *MMWR Morb. Mortal. Wkly. Rep.* 55:301–305.
4. Crofton, J., P. Chaulet, D. Maher, J. Grosset, W. Harris, H. Norman, M. Iseman, and B. Watt. 1997. Guidelines for the Management of Multidrug-Resistant Tuberculosis. World Health Organization: Geneva, Switzerland.
5. Katoch, K., M. Natarajan, A.S. Bhatia, and V.S. Yadav. 1992. Treatment of paucibacillary leprosy with a regimen containing rifampicin, dapsone and prothionamide. *Indian J. Lepr.* 64:303–312.
6. Banerjee, A., E. Dubnau, A. Quemard, V. Balasubramanian, K.S. Um, T. Wilson, D. Collins, G. de Lisle, and W.R. Jacobs Jr. 1994. inhA, a gene encoding a target for isoniazid and ethionamide in *Mycobacterium tuberculosis*. *Science*. 263:227–230.
7. Rozwarski, D.A., G.A. Grant, D.H. Barton, W.R. Jacobs Jr., and J.C. Sacchettini. 1998. Modification of the NADH of the isoniazid target (InhA) from *Mycobacterium tuberculosis*. *Science*. 279:98–102.
8. Vilcheze, C., F. Wang, M. Arai, M.H. Hazbon, R. Colangeli, L. Kremer, T.R. Weisbrod, D. Alland, J.C. Sacchettini, and W.R. Jacobs Jr. 2006. Transfer of a point mutation in *Mycobacterium tuberculosis* inhA resolves the target of isoniazid. *Nat. Med.* 12:1027–1029.
9. Takayama, K., L. Wang, and H.L. David. 1972. Effect of isoniazid on the in vivo mycolic acid synthesis, cell growth, and viability of *Mycobacterium tuberculosis*. *Antimicrob. Agents Chemother.* 2:29–35.
10. Winder, F.G., P.B. Collins, and D. Whelan. 1971. Effects of ethionamide and isoxyl on mycolic acid synthesis in *Mycobacterium tuberculosis* BCG. *J. Gen. Microbiol.* 66:379–380.
11. Wilson, T.M., G.W. de Lisle, and D.M. Collins. 1995. Effect of inhA and katG on isoniazid resistance and virulence of *Mycobacterium bovis*. *Mol. Microbiol.* 15:1009–1015.
12. Larsen, M.H., C. Vilcheze, L. Kremer, G.S. Besra, L. Parsons, M. Salfinger, L. Heifets, M.H. Hazbon, D. Alland, J.C. Sacchettini, and W.R. Jacobs Jr. 2002. Overexpression of inhA, but not kasA, confers resistance to isoniazid and ethionamide in *Mycobacterium smegmatis*, *M. bovis* BCG and *M. tuberculosis*. *Mol. Microbiol.* 46:453–466.
13. Morlock, G.P., B. Metchock, D. Sikes, J.T. Crawford, and R.C. Cooksey. 2003. ethA, inhA, and katG loci of ethionamide-resistant clinical *Mycobacterium tuberculosis* isolates. *Antimicrob. Agents Chemother.* 47:3799–3805.
14. Dessen, A., A. Quemard, J.S. Blanchard, W.R. Jacobs Jr., and J.C. Sacchettini. 1995. Crystal structure and function of the isoniazid target of *Mycobacterium tuberculosis*. *Science*. 267:1638–1641.
15. Johnsson, K., and P.G. Schultz. 1994. Mechanistic Studies of the Oxidation of Isoniazid by the Catalase Peroxidase from *Mycobacterium tuberculosis*. *J. Am. Chem. Soc.* 116:7425–7426.
16. Lei, B., C.J. Wei, and S.C. Tu. 2000. Action mechanism of antitubercular isoniazid. Activation by *Mycobacterium tuberculosis* KatG, isolation, and characterization of inha inhibitor. *J. Biol. Chem.* 275:2520–2526.
17. Johnsson, K., D.S. King, and P.G. Schultz. 1995. Studies on the Mechanism of Action of Isoniazid and Ethionamide in the Chemotherapy of Tuberculosis. *J. Am. Chem. Soc.* 117:5009–5010.
18. Zhang, Y., B. Heym, B. Allen, D. Young, and S. Cole. 1992. The catalase-peroxidase gene and isoniazid resistance of *Mycobacterium tuberculosis*. *Nature*. 358:591–593.
19. Fattorini, L., E. Iona, M.L. Ricci, O.F. Thoresen, G. Orru, M.R. Oggioni, E. Tortoli, C. Piersimoni, P. Chiaradonna, M. Tronci, et al. 1999. Activity of 16 antimicrobial agents against drug-resistant strains of *Mycobacterium tuberculosis*. *Microb. Drug Resist.* 5:265–270.
20. DeBarber, A.E., K. Mdluli, M. Bosman, L.G. Bekker, and C.E. Barry III. 2000. Ethionamide activation and sensitivity in multidrug-resistant *Mycobacterium tuberculosis*. *Proc. Natl. Acad. Sci. USA*. 97:9677–9682.
21. Baulard, A.R., J.C. Betts, J. Engohang-Ndong, S. Quan, R.A. McAdam, P.J. Brennan, C. Locht, and G.S. Besra. 2000. Activation of the pro-drug ethionamide is regulated in mycobacteria. *J. Biol. Chem.* 275:28326–28331.
22. Fraaije, M.W., N.M. Kamerbeek, A.J. Heidekamp, R. Fortin, and D.B. Janssen. 2004. The prodrug activator EtaA from *Mycobacterium tuberculosis* is a Baeyer-Villiger monooxygenase. *J. Biol. Chem.* 279:3354–3360.
23. Vannelli, T.A., A. Dykman, and P.R. Ortiz de Montellano. 2002. The antituberculosis drug ethionamide is activated by a flavoprotein monooxygenase. *J. Biol. Chem.* 277:12824–12829.
24. Quemard, A., G. Laneelle, and C. Lacave. 1992. Mycolic acid synthesis: a target for ethionamide in mycobacteria? *Antimicrob. Agents Chemother.* 36:1316–1321.
25. Tokuyama, H., T. Yamashita, M.T. Reding, Y. Kaburagi, and T. Fukuyama. 1999. Radical Cyclization of 2-Alkenylthioanilides: A Novel Synthesis of 2,3-Disubstituted Indoles. *J. Am. Chem. Soc.* 121:3791–3792.
26. Vilcheze, C., T.R. Weisbrod, B. Chen, L. Kremer, M.H. Hazbon, F. Wang, D. Alland, J.C. Sacchettini, and W.R. Jacobs Jr. 2005. Altered NADH/NAD+ ratio mediates coresistance to isoniazid and ethionamide in mycobacteria. *Antimicrob. Agents Chemother.* 49:708–720.
27. McPherson, A. 1982. Preparation and Analysis of Protein Crystals. John Wiley & Sons Inc., New York. 371 pp.
28. Otwinowski, Z., and W. Minor. 1997. Processing of x-ray diffraction data collected in oscillation mode. *In* Methods in Enzymology. C.W. Carter and R.M. Sweet, editors. Academic Press, New York. 307–326.
29. Brunger, A.T., P.D. Adams, G.M. Clore, W.L. DeLano, P. Gros, R.W. Grosse-Kunstleve, J.S. Jiang, J. Kuszewski, M. Nilges, N.S. Pannu, et al. 1998. Crystallography & NMR system: A new software suite for macromolecular structure determination. *Acta Crystallogr. D Biol. Crystallogr.* 54:905–921.
30. McRee, D.E. 1999. XtalView/Xfit–A versatile program for manipulating atomic coordinates and electron density. *J. Struct. Biol.* 125:156–165.